Error Estimation of Discrete Geometry Method on Plasmonic Structures

Shuai Yan[1], Xiaoyu Xu[1], Christoph Pflaum[2], Zhuoxiang Ren[1,3]
[1]Institute of Microelectronics, Chinese Academy of Sciences,
Beijing, 100029, China, yanshuai@ime.ac.cn
[2]Chair of systemsimulation, Department of Computer Science, Friedrich-Alexander-Universität Erlangen-Nürnberg,
Erlangen, 91058, Germany, christoph.pflaum@fau.de
[3]Sorbonne Universités, UPMC Univ. Paris 06, 75005 Paris, France, zhuoxiang.ren@upmc.fr

We derive the local and global discretization error of the discrete geometry method (DGM) on a plasmonic structure. Based on a structured discretization of the computational domain, two cases of field distributions are considered: one with electric field distributed on primal mesh and magnetic field on dual mesh, the other conversely. The analysis shows that when the magnetic field is placed on primal mesh, the numerical scheme approximates the continuous problem better than the case when electric field are placed on primal mesh. The convergence rate for both cases are calculated.

Index Terms—**Computational electromagnetic, convergence of numerical methods, discrete geometry method, surface plasmons.**

I. Introduction

Plasmonics are defined by the interacting processes between the electromagnetic waves and the conducting electrons at metallic interfaces or nanostructures, which leads to an enhanced optical near field of sub-wavelength dimension. In recent years, accompanied with the development of nano fabrication techniques, surface plasmon shows its potential in a large variety of applications [1]. Plasmonics bring singularities to solutions of Maxwell's equations at the metallic interfaces [2]. In another word, the solution is not classical since it has no strong derivatives at the metallic interfaces. Therefore, it is necessary to revisit the error estimation results for commonly used numerical methods, since for most cases, these results are based on Taylor expansions of the electromagnetic fields. The local singularities can cause additional error in the expanded terms. It is important to assure that the discrete approximations are still consistent to the continuous Maxwell's system in spite of the local singularities.

Discrete geometry method (DGM) is based on a differential geometry interpretation of the Maxwell's system. Within this framework, different kinds of finite methods including finite difference time domain (FDTD) method, finite integrate techniques (FIT) and finite element method (FEM) can be unified in a general form (1)-(3) ([3], [4]).

$$C^T\mathbf{h} = d_t\mathbf{d} + \mathbf{j} \tag{1}$$

$$C\mathbf{e} = -d_t\mathbf{b} \tag{2}$$

$$\mathbf{d} = M_\epsilon\mathbf{e}, \mathbf{b} = M_\mu\mathbf{h}, \mathbf{j} = M_\sigma\mathbf{e}. \tag{3}$$

e, **h**, **b**, **d** and **j** are the line or surface integrals of electric field **E**, magnetic field **H**, electric flux density **D**, magnetic flux density **B**, and electric current density **J** respectively, C is the discrete version of the curl operator and d_t denotes the time derivative. With this algebraic form, (1) and (2) keep the "metric-free" nature of Faraday's law and Ampere's law. The metric information is condensed in the constitutive matrices M_ϵ, M_μ and M_σ in (3). The three constitutive matrices actually give discretization to the continuous Hodge operator that maps 1-differential forms to 2-differential forms in E^3 space. Thus, no matter how a discrete method is derived, it is only distinct from other methods in the manner to discretize the Hodge operator. DGM construct the constitutive matrices by a physically natural way ([4], [5]). This enables a numerical scheme that possesses the main advantages of both FDTD/FIT (diagonal constitutive matrices) and FEM (can be applied on unstructured mesh).

II. Surface Plasmon Polaritons

Surface plasmon polariton (SPP) is a propagating evanescent wave along the metallic/dielectric interfaces. The most simple geometry sustaining SPP is a single, flat interface between a dielectric, non-absorbing half space with positive real dielectric constant ϵ_d and an adjacent conducting half space with a dielectric function $\epsilon_m(\omega) = \epsilon_{m,r}(\omega) + i\epsilon_{m,i}(\omega)$. The requirement of metallic character implies $\epsilon_{m,r}(\omega) < 0$. The analytical solution is available for this simple geometry [1].

$$\begin{cases} \hat{H}_y(x,y,z) &= Ae^{-k_d(z-z_0)}e^{i\beta x} \\ \hat{E}_x(x,y,z) &= -iA\frac{1}{\omega\epsilon_0\epsilon_d}k_d e^{-k_d(z-z_0)}e^{i\beta x} \\ \hat{E}_z(x,y,z) &= A\frac{\beta}{\omega\epsilon_0\epsilon_d}e^{-k_d(z-z_0)}e^{i\beta x} \end{cases}, \text{ when } z > z_0 \tag{4}$$

$$\begin{cases} \hat{H}_y(x,y,z) &= Ae^{k_m(z-z_0)}e^{i\beta x} \\ \hat{E}_x(x,y,z) &= iA\frac{1}{\omega\epsilon_0\epsilon_m}k_m e^{k_m(z-z_0)}e^{i\beta x} \\ \hat{E}_z(x,y,z) &= A\frac{\beta}{\omega\epsilon_0\epsilon_m}e^{k_m(z-z_0)}e^{i\beta x} \end{cases}, \text{ when } z \le z_0 \tag{5}$$

The hat indicates that the fields here are time-harmonic components of the original electric and magnetic fields. the complex "wave number" of SPP β takes the value $\beta = k_0\sqrt{\frac{\epsilon_m\epsilon_d}{\epsilon_m+\epsilon_d}}$. and k_m and k_d are related to the dielectric constants by $k_m/k_d = -\epsilon_m/\epsilon_d$. A demonstration of the solution is shown in Fig. 1. The field is enhanced at the dielectric/metallic interface and decreases evanescently in both materials.

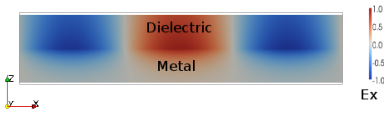

Fig. 1. A demonstration of the time harmonic SPP solution.

III. Error Expression and Estimation

Let $\mathbf{e}^*$, $\mathbf{h}^*$, $\mathbf{d}^*$, $\mathbf{b}^*$ and $\mathbf{j}^*$ be the exact solutions of the maxwell's system. On the discrete mesh, they fulfill a linear system as follows:

$$C^T\mathbf{h}^* = d_t\mathbf{d}^* + \mathbf{j}^* \tag{6}$$

$$C\mathbf{e}^* = -d_t\mathbf{b}^* \tag{7}$$

$$\mathbf{d}^* = M_\epsilon\mathbf{e}^* + R_\epsilon, \mathbf{b}^* = M_\mu\mathbf{h}^* + R_\mu, \mathbf{j}^* = M_\sigma\mathbf{e}^* + R_\sigma, \tag{8}$$

where R_ϵ, R_μ and R_σ are errors on constitutive laws. Let $\mathbf{r^e} = \mathbf{e}^* - \mathbf{e}$ and $\mathbf{r^h} = \mathbf{h}^* - \mathbf{h}$, and subtract (1)-(3) from (6)-(8), we can get the following system.

$$C^T\mathbf{r^h} = i\omega M_\epsilon\mathbf{r^e} + M_\sigma\mathbf{r^e} + i\omega R_\epsilon + R_\sigma \tag{9}$$

$$C\mathbf{r^e} = -i\omega M_\mu\mathbf{r^h} + i\omega R_\mu. \tag{10}$$

Note that the time dependency is removed by the time-harmonic assumption. We use the same expressions without ambiguity. Solving out $\mathbf{r^e}$ from (9) and substituting it into (10) yields

$$\mathbf{r^h} - \omega^2 M_\mu^{-1}C(M_\epsilon + \frac{M_\sigma}{i\omega})^{-1}C^T\mathbf{r^h} = \mathbf{R} \tag{11}$$

with the truncation error of the system defined by

$$\mathbf{R} = M_\mu^{-1}R_\mu - \omega^2 M_\mu^{-1}C(M_\epsilon + \frac{M_\sigma}{i\omega})^{-1}(i\omega R_\epsilon + R_\sigma). \tag{12}$$

We consider a two-dimensional computational domain with the simple SPP structure mentioned in Sec. II. The domain is located on the x-z plane and discretized by an uniform Yee's Grid with mesh size (h_x, h_z). We calculate $\mathbf{R}$ for two kinds of field distributions: one with electric components on the primal mesh and magnetic components on the dual mesh, and the other conversely. The metallic and dielectric interface is located on the primal mesh. A geometry demonstration is given in Fig. 2. For any homogeneous dual pair $(L_m^{(p)}, A_m^{(d)})$ in case 1 or $(A_m^{(p)}, L_m^{(d)})$ in case 2, the corresponding diagonal component $(M_\epsilon)_{m,m}$ is calculated by $(M_\epsilon)_{m,m} = \epsilon\frac{|A_m^{(d)}|}{|L_m^{(p)}|}$ or $(M_\epsilon)_{m,m} = \epsilon\frac{|A_m^{(p)}|}{|L_m^{(d)}|}$. M_σ is defined similarly and M_μ are defined dually following the same way . Therefore, given any degree of freedom $\mathbf{h}$ locating at least one cell away from the interface, the local truncation error $\mathbf{R}$ can be easily evaluated as $O(h_x^2 + h_z^2)$.

We then come to the situation when the interface involves. Consider the edge locating at the interface in case 1 and the one intersecting the interface in case 2. (marked in green in Fig. 2). We denote both their indexes by m_0. Taking M_ϵ as an example, its corresponding diagonal components are calculated by

$$(M_\epsilon)_{m_0,m_0} = \frac{\epsilon_d|A_1^{(d)}|}{|L^{(p)}|} + \frac{\epsilon_m|A_2^{(d)}|}{|L^{(p)}|} \quad \text{(Case 1)} \tag{13}$$

$$(M_\epsilon)_{m_0,m_0} = \frac{\epsilon_d\epsilon_m|A^{(p)}|}{\epsilon_d|L_2^{(d)}| + \epsilon_m|L_1^{(d)}|} \quad \text{(Case 2)} \tag{14}$$

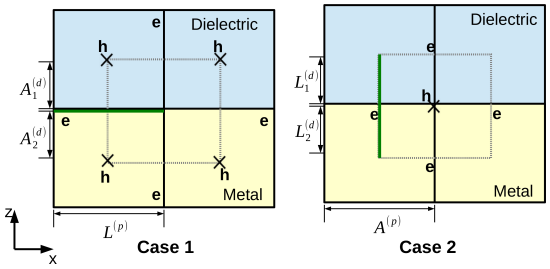

Fig. 2. A demonstration of two kinds of field distribution at the metallic interface.

We then evaluate the errors R_ϵ, R_σ and R_μ according to (8) with the exact solutions given in (4) and (5). We apply the Taylor expansion and cancel out the low order terms to get the order of the error terms. Furthermore, we evaluate the two subtraction terms of $\mathbf{R}$ in (12), and the results are presented in Table. I. For both cases, the error with respect to h_z is dominant. In case 1, the truncation error is a constant at the interface. Therefore, the numerical approximation is inconsistent to the continuous problem in the L_∞ sense. And in case 2, the consistency is fulfilled with a convergence rate of $O(h_z)$. In a weaker L_2 sense, however, consistency can also be fulfilled with an order of $O(h_z^{1/2})$ for case 1. Additionaly, we need to remark here that the calculation of $\mathbf{R}$ relies on the fact that the constitutive matrices are diagonal. For implicit methods as FEM, the evaluation of 12 involves two invertion of large matrices, so that it gets much more complicated and expensive.

TABLE I
Truncation error at the interface.

	First term in (12)	Second term in (12)
Case 1	$O(h_x^2) + O(h_z^2)$	$O(h_x^2) + O(1)$
Case 2	$O(h_x^2) + O(h_z)$	$O(h_x^2) + O(h_z)$

IV. Conclusion

In this paper, we study the influence of field singularity to the truncation error of DGM on a plasmonic structure for two different kinds of discretization. The analysis can guide the simulation of the plasmonic behavior with DGM on more complex structures. Details of the calculation and numerical examples will be presented in the full paper.

Acknowledgement

This work was partially supported by the National Science Foundation of China (No. 51407181) and the Director Foundation of Institute of Microelectronics of Chinese Academy of Sciences (No. Y3SZ0701).

References

[1] S. A. Maier, *Plasmonics: Fundamentals and Applications.*, Springer, 2007.

[2] A. Mohammadi, T. Jalali, and M. Agio, *Dispersive contour-path algorithm for the two-dimensional finite-differencetime-domain method.* Opt. Express (16), 2008.

[3] M. Clemens and T. Weiland, *Discrete Electromagnetism with the Finite Integration Technique.*, Prog. Electromagn. Res.(32), 2011.

[4] A. Bossavit, *'Generalized Finite Differences' in Computational Electromagnetics.*, Prog. Electromagn. Res. (15), 2011.

[5] Z. Ren and X. Xu, *Dual Discrete Geometric Methods in Terms of Scalar Potential on Unstructured Mesh in Electrostatics.*, IEEE T. Mag.(50), 2014.